

Boundary-bulk interplay of molecular motor traffic flow through a compartment

M. Ebrahim Fouladvand (1,2), Modjtaba Salehi (1) and Mostafa Yadegari (1)

(1) Department of Physics, Zanjan University, P.O. Box 45196-313, Zanjan, Iran.

(2) Department of Nano-Science, Institute for Studies in Theoretical Physics and Mathematics (IPM), P.O. Box 19395-5531, Tehran, Iran.

The flow of motor proteins on a filamental track is modelled within the the framework of lattice driven diffusive systems. Motors, considered as hopping particles, perform a highly biased asymmetric exclusion process when bound to the filament. With a certain rate, they detach from the filament and execute unbiased random walk in the bulk which is considered as a closed cubic compartment. Motors are injected (extracted) from the leftmost (rightmost) site of the filament located along the symmetry axis of the compartment. We explore the transport properties of this system and investigate the bulk-boundary interplay on the system stationary states. It is shown that the detachment rate notably affects the system properties. In particular and in contrast to ASEP, it is shown that the density profile of bound particles exhibit different types of non monotonic behaviours when the detachment rate varies. It is shown that in certain situations, the density profile of the filament consists of coexisting high and low regions.

PACS numbers: 02.50.Ey, 05.40.-a, 05.70.Ln, 64.60.-i

I. INTRODUCTION

Many transport problems in physics and related interdisciplinary areas have been successfully modelled within the framework of lattice driven diffusive systems. The kinetics of biopolymerization¹⁻³, interface growth,^{2,4} and vehicular traffic flow⁵⁻⁷ are among various examples of diverse applications of cellular automaton approach in describing out of equilibrium systems. Driven lattice gases with open boundaries are stochastic lattice models of particles which hop preferentially in one direction and which are connected at their boundaries to particle reservoirs of constant densities. As a result of this coupling, a stationary flow of particles is established in the system. A prototype example of non-equilibrium low dimensional systems is the asymmetric simple exclusion process (ASEP) where particles interact through hard-core repulsion⁸. ASEP has been applied to describe a variety of phenomena in physics and beyond. In one dimension, many interesting feature such as boundary-induced phase transitions, spontaneous symmetry breaking and shock formation have been shown to exist⁹⁻¹³. These phenomena are associated to the boundary effects on the chain bulk and are generally termed *boundary induced*. Besides the boundaries, the bulk properties of the 1D chain can be affected via coupling to a 3D bulk reservoir. A well known example is the *Langmuir kinetics* (LK)¹⁴ where particles can adsorb (desorb) if a bulk site is empty (occupied). Recently the interplay of both effects i.e., the boundary and the bulk reservoirs have received attention¹⁵⁻¹⁸. It has been verified that in certain situations where the adsorption/desorption rate properly scales with the system size, the density profile exhibits a non-monotonic structure in the bulk which is

characterized by the coexistence of low and high density regions separated by a shock front if the system size is high enough. In contrast to ASEP where shocks are not localized, in the presence of adsorption/desorption of particles, the system shows a more complex and richer behaviour. Specially, the shocks are localized. This behaviour can be verified by a continuous mean-field approach¹⁵⁻¹⁷. Along this line of study, we investigate the bulk-boundary interplay in a one dimensional chain. In our study, the homogeneous bulk reservoir is replaced by a more realistic structure. More specifically, the bound particles can detach from the one dimensional chain and execute unbiased random walk. The unbound particles are confined to a compartment with reflecting boundaries. It is one of our main objectives to see how the cooperative behaviours of the diffusive unbound particles affects the results obtained from the static homogeneous 3D bulk. We are interested to know if the shock localisation persists in the case where the bulk particles have dynamics. Our study is motivated from a biological application of ASEP. A considerable portion of intra-cell transport of biological cargos in eucaryotic cells is performed via the so-called motor proteins namely kinesin, myosin and dynein which move on filamentary tracks called microtubules and actins¹⁹⁻²⁶. These bio motors perform a biased processive random walk on the filament and after some while detach from it due to thermal noise. Recently some physicists have attempted to formulated the problem described above within the lattice driven gas framework²⁷⁻³¹. Besides investigating the diffusion properties of a single molecular motor on a filament-like track, these investigations have been generalized to account for the mutual interaction of motors via hard core repulsion. The interaction was considered at its simplest form i.e., *exclusion*. It has been shown that anisotropy induced

by the filament can affect the diffusion properties of the bulk particles which are unbound to the filament. On the other hand, the bulk diffusive motors can substantially influence the structure of the density and current profiles on the filament. It has been recently shown³² that in a compartment containing cytoskeletal filaments, hard core interaction between unbound motors, which are confined to move inside the compartment, and the filament gives rise to a localized shock structure in the density profile of the filament. The above geometrical arrangement i.e., a filament placed along the symmetry axis of a compartment are accessible to *in vitro* experiments and mimics the structure observed in cytoskeleton. In particular, such systems serve as simple models for the description of motor-based transport in an axon^{34,35}. In this paper our main focus is on the role of detachment rate on the filament density profile. The investigation of the consequences of changing the detachment rate can be important not only from biological but also for theoretical purposes.

II. DESCRIPTION OF THE PROBLEM AND ITS FORMULATION

Before proceeding further into the problem, let us define the model in more details. The motor proteins motion is assumed to take place in a compartment. For simplicity, we take the compartment shape a three dimensional cube with dimensions Lx, Ly and Lz in the directions x, y and z respectively. We assume the filament is located along the x axis of the tube. Furthermore, the filament coordinates in y and z directions are taken as $y = \frac{Ly}{2}$ and $z = \frac{Lz}{2}$. We assume the particles (motors) enter onto the filament from the left boundary i.e., at the point $(x, y, z) = (0, \frac{Ly}{2}, \frac{Lz}{2})$. The particles can leave the compartment only via reaching the last point of the filament which is $(x, y, z) = (Lx, \frac{Ly}{2}, \frac{Lz}{2})$. The particles movement are governed according the following discrete-time stochastic dynamical rules. At each time step t , the state of the system is specified by the occupation numbers of each site inside the compartment. If the site is full, its occupation number is one. If it is empty, the occupation number is zero. In addition, the motors are assumed to be point particles. Note that the integer coordinates i, j and k of the sites are restricted as $0 \leq i \leq Lx$; $0 \leq j \leq Ly$; $0 \leq k \leq Lz$. Now we explain the updating rules applied to all the particles inside the compartment.

1) particle injection:

In the beginning of the time step, we update the entry site of the filament: if the first site of the filament is empty, a particle will be injected to it with the probability α . Furthermore, The number of entrants will be regarded as the system inflow.

2) bound particle movement:

We divide the particles inside the compartment into two groups: bound and unbound. If the particle is on the filament, we consider it as a bound one. If it is outside the filament, it is regard as an unbound particle. As discussed, the filament role is to provide a driven track on which the particles diffusive motion is highly directed. A particle on the filament can randomly move one step forward with probability p , one step backward with probability δ , remains immobile at its position with probability γ or leave the filament (detachment) to one of its non-filament neighbours with probability $\frac{\epsilon}{6}$ ^{29,30}. All these random movements will be successful if the target site is empty. In case the target site is already occupied by another motor, the attempted hop will be rejected. The probabilities should sum up to one: $p + \delta + \gamma + \frac{2\epsilon}{3} = 1$. In three dimensions, there are four neighbouring non-filament sites adjacent to each filament site $(i, \frac{Ly}{2}, \frac{Lz}{2})$ therefore the detachment probability equals $\frac{2\epsilon}{3}$.

3) unbound particle movement:

An unbound particle is the one which is not located on the filament. These particles diffuse freely in the compartment space until they find a chance to attach to the filament. Once they attach to the filament, they become bound. The diffusion probabilities to the adjacent empty sites are equally taken to be $\frac{1}{6}$ for all six spatial directions. For unbound particles, the compartment boundaries are assumed to be totally reflective. This can be implemented by putting immobile particles on the all boundary sites expect the entrance site $(0, \frac{Ly}{2}, \frac{Lz}{2})$ and the exit site $(Lx, \frac{Ly}{2}, \frac{Lz}{2})$.

4) particle extraction:

Once a bound particle reaches the last filament site, it will be removed from the system (compartment) with the exit probability β . The number of removed particles will be regarded as the system outflow. We recall that due to binding/unbinding of particles from the filament, in the steady state the current depends on the filament site number. Throughout this paper by current we mean the current of the last filament site.

updating scheme:

Before proceeding further, it would be illustrative to discuss, in some details, the type of our updating. Basically, in the CA (cellular automata) models, the updating schemes are divided into two categories: *particle-oriented* and *site-oriented*. The particle oriented scheme can itself be divided into various methods. The most important one is parallel dynamics in which the updating rules are synchronously applied to all particles. The prototype ex-

ample is the vehicular traffic flow⁵. The next variant is the ordered sequential updating. In this scheme, one updates the particles in an ordered sequential manner say from left to right in one dimensional open systems. Finally the third type is random sequential update. In this scheme, an update step is composed of many sub-update steps. In each sub-update step, we randomly chose one of the particles and update its position in accordance to the movement rules. In contrast to particle-oriented schemes, one has site-oriented ones. Site-oriented schemes, are generically divided into ordered and random sequential types. In the ordered scheme, one sweeps the lattice in a certain direction (prescribed by the method) and updates the position of those sites which are occupied by particles. In random sequential type, one randomly selects a site. If this site is occupied, then updating is done otherwise one continues by selecting other sites until an occupied site is found. The type of updating will affect some aspects of the problem but normally the phase structure of the model will not substantially changed under changing the updating scheme. In this paper we use particle-oriented ordered sequential scheme. More specifically, we label each particle upon entering into the compartment. At each time step, we update the particles' positions in the order of their labels. This resembles the site-ordered random sequential update. Our motivation to choose this update stems from our interest to evaluate the passage time of particles from entrance to removal. In the following sections we present our simulation results and discuss the phase structure and the other statistical properties of this system.

III. SIMULATION RESULTS

If we allow time to evolve for a long time we see the systems reaches a non-equilibrium current-carrying steady state in which the statistical properties of the system does not show significant changes with time. To see this more explicitly, let us first define the quantities we are interested to compute:

1) number of bound particles at the end of timestep t denoted by $N_b(t)$. The subscript b denotes *bound*. Dividing $N_b(t)$ by the filament size Lx gives the instantaneous global filament density at time t which we denote it by $\rho_b(t)$.

2) number of unbound particles at the end of timestep t denoted by $N_{ub}(t)$. Dividing $N_{ub}(t)$ by the compartment volume $Lx \times Ly \times Lz - Lx$ gives the unbound global particle density at time t which we denote it by $\rho_{ub}(t)$.

3) filament current $J_b(t)$ which is defined to be the number of particle exited from the last filament site by the end of t -th step divided by t .

4) passage time of each particle: since we label the particles upon entering into the system, we can follow their trajectories from the time they enter the compartment until the time they leave it. Therefore we can specify each particle's passage time. $p(t)$ is defined to be the average passage time of those particles which have already exited the compartment by the end of time t .

5) centre of mass of the unbound particles denoted by $\langle X_{ub} \rangle(t)$. This quantity is obtained by averaging over the x -coordinate of all unbound particles at time t .

6) centre of mass of the bound particles denoted by $\langle X_b \rangle(t)$. This quantity is obtained by averaging over the x -coordinate of all bound particles at time t .

7) total number of particles in the system i.e., $N_{ub}(t) + N_b(t)$ which is named *load*.

We note that in the steady state, the radial current of particles onto the filament should be equal to the current of particles leaving the filament. This is called *radial equilibrium* discussed in^{29,30}. In a mean-field approximation, the radial equilibrium implies the following relationship between ρ_b and ρ_{ub} :

$$\frac{\epsilon}{6}\rho_b(1 - \rho_{ub}) = \frac{1}{6}\rho_{ub}(1 - \rho_b) \quad (1)$$

In the following we exhibit the stationary characteristics of the system. The system contains $Lx = 100$ sites. The perpendicular dimensions are $Ly = Lz = 25$ and $\delta = \gamma = 0$ unless otherwise specified. In the first figure, we sketch the dependence of steady-state value of load in terms of α for three values of detachment rate ϵ and exit rate β .

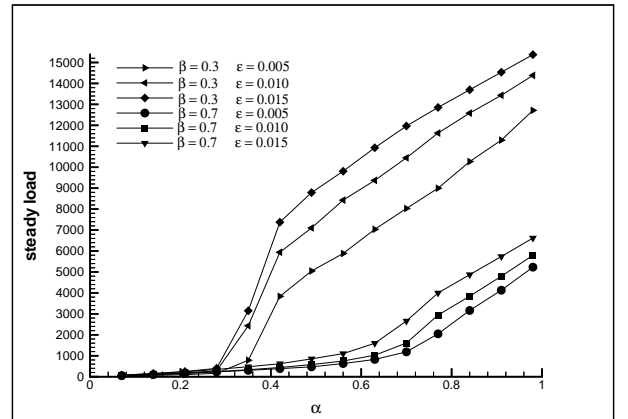


Fig. 1: steady state value of load vs α . ϵ and β are specified in the figure.

We observe a phase-transition like behaviour near $\alpha_c \sim 0.3$ and 0.7 , for $\beta = 0.3$ and 0.7 respectively, where the steady load shows up a sharp increase. Moreover, increasing ϵ gives rise to increment of the load. This is

expected since increasing ϵ raises the detachment probability hence the number of unbound particles is increased. To verify this transition, let us consider the dependence of the bound current J_b on α .

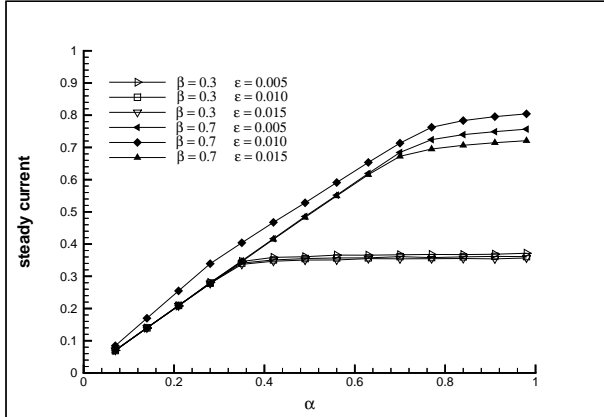


Fig. 2: steady state current in terms of α for a system of size $Lx = 100$. The value of β and ϵ are specified in the figure.

for $\beta = 0.3$ the current linearly increases with respect to α and then saturates at an ϵ -dependent value. The saturation value lies near 0.35. The smaller values of ϵ correspond to higher currents. This can be explained on account of the fact that for small ϵ motors prefer to remain bound to the filament track and continue their biased movement toward the exit point. Furthermore, we observe that the effect of increasing ϵ is smoothing the transition. For larger value of $\beta = 0.7$, the overall picture remains the same. However the transition point and saturation value changes correspondingly. These behaviour are analogous to ASEP. The next quantity is the passage time. We exhibit the steady state passage time vs α for some values of β and ϵ .

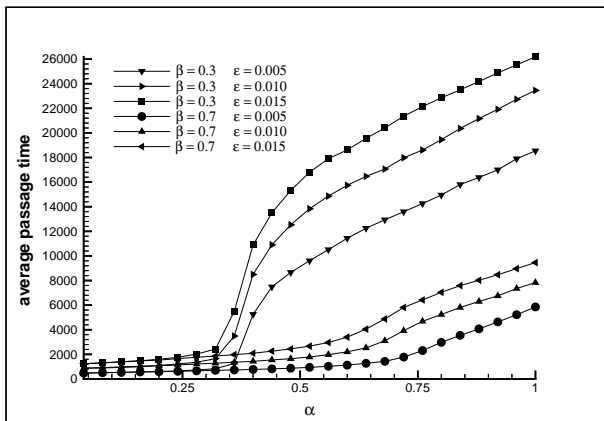


Fig. 3: steady state passage time in terms of α . $Lx = 100$ and the values of β and ϵ are specified in the figure.

The above graph is similar to the load graph. One can

see the phase transition is also manifested in the passage time. We note that transition is smooth for $\beta = 0.7$ and it resembles to a cross over. Let us next consider the density of bound motors ρ_b as a function of α .

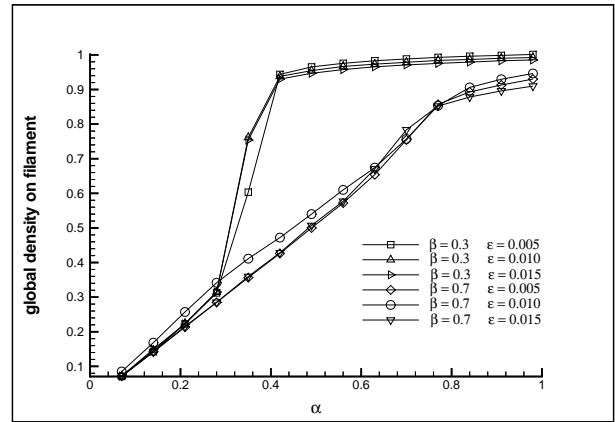


Fig. 4: steady state ρ_b in terms of α for a system of size $Lx = 100$. The values of β and ϵ are specified in the figure.

Again, one observes phase transition behaviour from a low to a high density phase for $\beta = 0.3$ but a smooth crossover-like behaviour for $\beta = 0.7$. The results for $\beta = 0.3$ i.e., a first order low-to-high density transition is similar to that of ASEP. However when $\beta = 0.7$ one observes slight differences to the behaviour of ASEP. Specifically, we see deviations from linear dependence of ρ_b vs α before reaching the saturation region. We also obtained the above diagram for $Lx = 200$ and 300 . The results are very close to the case $Lx = 100$. We next explore the properties of the average position of the bound motors $\langle x \rangle_b$. The behaviour of $\langle x \rangle_b$ in terms of α is exhibited in the next graph.

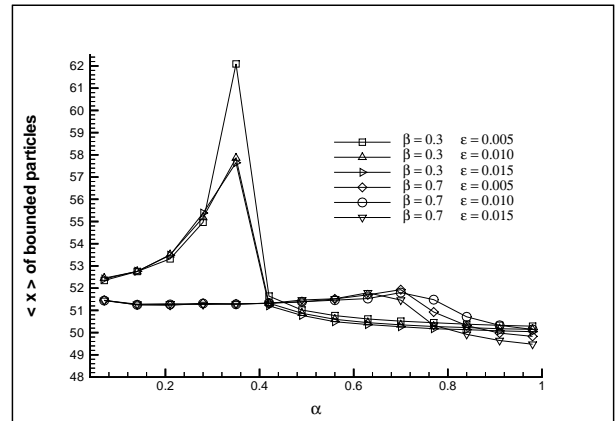


Fig. 5: steady state $\langle x \rangle_b$ in terms of α for a system of size $Lx = 100$. The value of β and ϵ are specified in the figure.

It is interesting to note that $\langle x \rangle_b$ reaches its peak

at the transition point but decreases afterwards. Before transition, the system's load as well as ρ_b are small and one does not expect jam formation hence $\langle x \rangle_b$ should be around half of the filament length (here 50). Near transition point, jams are formed near the exit point and correspondingly $\langle x \rangle_b$ increases over $\frac{L_x}{2} = 50$. The interesting point is that $\langle x \rangle_b$ starts decreasing with further increase of α . This could be related to the bulk effects due to unbound particles. For $\beta = 0.7$ this effect is suppressed and the sharp peak is smeared out. The appearance of a peak in the centre of mass of bound particles signifies an important characteristics. The peak tells us that around the value $\alpha \sim 0.35$ an inhomogeneous density structure forms throughout the filament. This point will become more clear by examining the filament density profile. To get a deeper insight, it would be useful to consider density profile on the filament. Figure (6) shows such profiles.

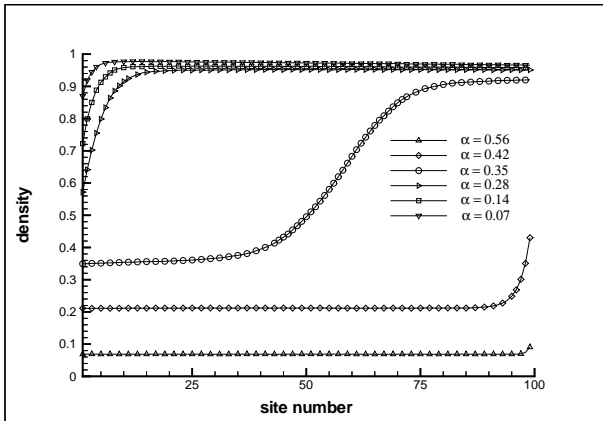


Fig. 6: density profile on the filament for various values of α for a system of size $L_x = 100$. $\beta = 0.3$ and $\epsilon = 0.005$.

For small values of ϵ , we observe analogous behaviour to ASEP. One has an exponential increase near the right boundary in the low density phase. In marked contrast to ASEP, we see that for α equal to 0.35, there is a coexistence of low and high density regions. In other words, there is a localized shock structure. This has been earlier reported when the bulk was modelled by constant attachment/detachment rates.¹⁵⁻¹⁷ Due to finite size of the system, the domain wall is not so sharp. Upon increasing α , the density again becomes nearly constant in the bulk with an exponential density decrease near the left boundary. To see the effect of varying ϵ , in the following figure, we have depicted the density profile for the same values of α but with $\epsilon = 0.015$.

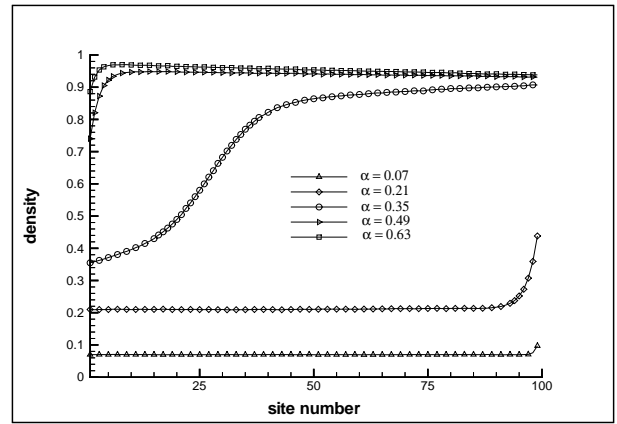


Fig. 7: density profile on the filament for various values of α for a system of size $L_x = 100$, $\beta = 0.3$ and $\epsilon = 0.015$.

Analogous to the case $\epsilon = 0.005$, we again have a localized shock structure at the same α but this time the position of the domain wall is shifted towards left. Furthermore, one can recognize a linear profile, with a small slope, in the high density regime. Although the slope is small but it is yet a distinguishing aspect. This can be related to formation of spontaneous jam or moving shocks and is a new feature of the problem which is absent in ASEP. In fact, the interaction of one dimensional filament with the unbound bulk particles leads to this weakly linear density profile. Now let us investigate the model properties when the exit rate β is changed. The following figure illustrates the behaviour of steady load vs β for $\alpha = 0.3$ and 0.7 each for three values of ϵ .

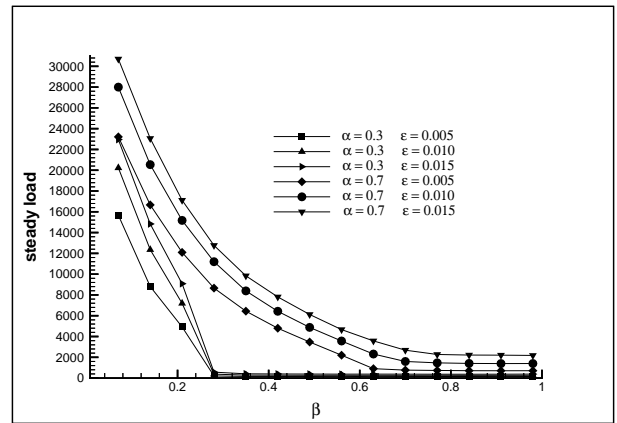


Fig. 8: steady state load vs β for a system of size $L_x = 100$ for various values of α and ϵ .

For $\alpha = 0.3$ one observes a transition-like behaviour while for larger $\alpha = 0.7$ the abrupt behaviour is changed into a smooth one. The effect of increasing ϵ is again smoothing the transition behaviour. The passage time diagram is similar to the load diagram and we do not show it. More interesting is the steady current behaviour.

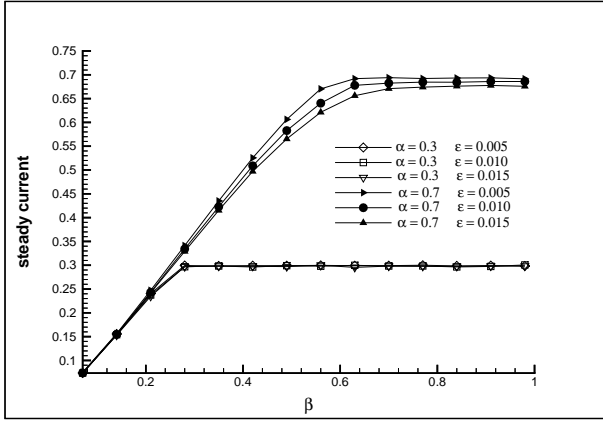


Fig. 9: steady state current in terms of β for a system of size $Lx = 100$. The value of α and ϵ are the same as in the previous figure.

Analogous to ASEP, the current saturates at a α -dependent value. The effect of ϵ is notable only for high α , corresponding to high density phase, where its increase gives rise to a current decline as expected. Besides this feature, for high α we see that varying ϵ gives rise to smoothing of the changes in the current. Next we look at the global density on the filament. The following graph depicts this behaviour.

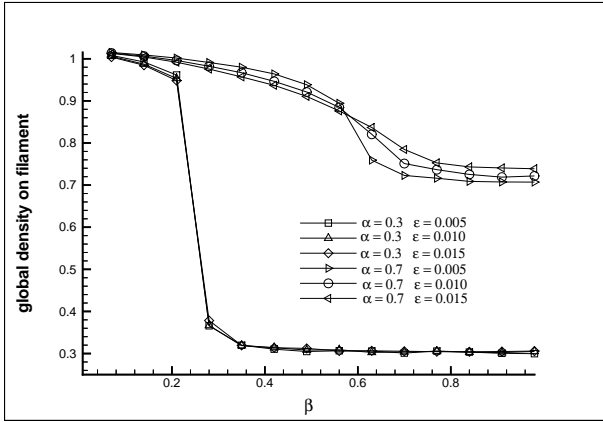


Fig. 10: steady state ρ_b in terms of β for a system of size $Lx = 100$. The value of α and ϵ are specified in the figure.

Similar to ASEP, one observes a first order high-to-low density transition for $\alpha = 0.3$ and a smoothly decreasing behaviour for $\alpha = 0.7$ until it reaches a constant value. The transition occurs at $\beta \sim 0.25$. We also examined the case $Lx = 200$ and 300 . The results do not show significant changes to the case $Lx = 100$. This shows that the behaviour is not due to finite size effects but is related to the bulk influence. We have also evaluated the $\langle x \rangle_b$ i.e., the average position of bound particles vs β . Figure (11) shows this dependence.

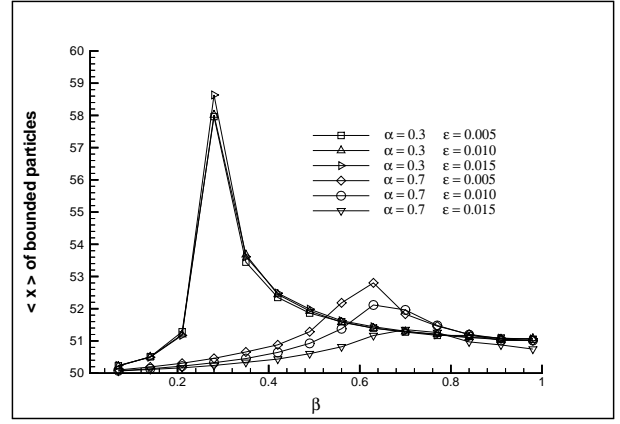
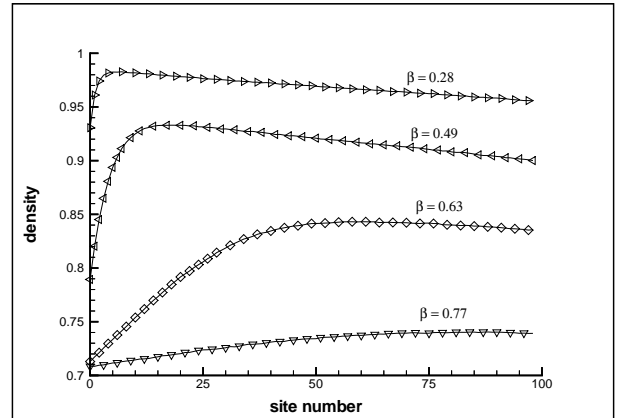
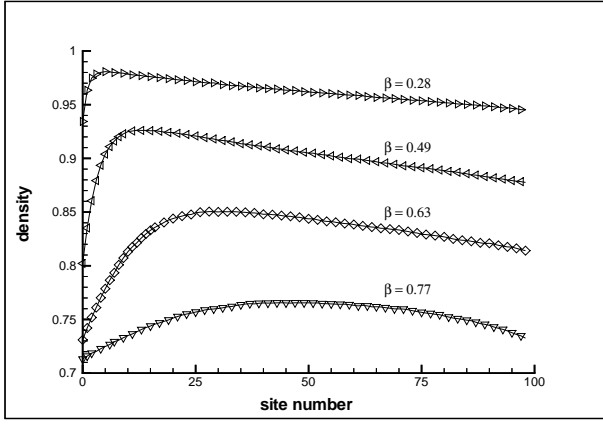


Fig. 11: steady state $\langle x \rangle_b$ in terms of β for a system of size $Lx = 100$. The value of α and ϵ are specified in the figure.

Similar to figure (5), we see a sharp increase of $\langle x \rangle_b$ to a maximum value $\sim 0.6Lx$ at the transition point. It decreases to half of the filament for larger values of β . The position of maximum crucially depends on α and ϵ . For larger values of α , the maximum point shifts towards larger β . Moreover, the maximum value of $\langle x \rangle_b$ reduces. The reason is that for larger α , the system contains more particles and can maintain high current. This leads to a more homogenised density profile. Lastly, we depict the density profiles for some values of β with $\epsilon = 0.01$ and 0.015 in the following figures. In comparison to ASEP, we see entirely different profiles. Generally, the profile is increased and then starts declining in a linear manner.



Figs. 12: density profile on the filament for various values of β for a system of size $Lx = 100$ and $\alpha = 0.7$. $\epsilon = 0.01$.



Figs. 13: density profile on the filament for various values of β for a system of size $Lx = 100$ and $\alpha = 0.7$. $\epsilon = 0.015$.

The effect of increasing β is two fold. First, smoothing the changes between increasing and decreasing regions of the density profile and second, extending the region of increasing profile. In comparison to the top figure where $\epsilon = 0.01$, for a larger value of $\epsilon = 0.015$ we see that the size of region where the profile is increasing, decreases. Increasing ϵ is more effective when the exit rate β is large. For instance, when $\beta = 0.63$, the increasing part of the density profile decreases in comparison to the case $\epsilon = 0.005$.

To see the behaviour of the density profile for larger systems size, we also obtained the profile for the same parameters as in the above figures but this time for $Lx = 300$. The following figure depicts the behaviour:

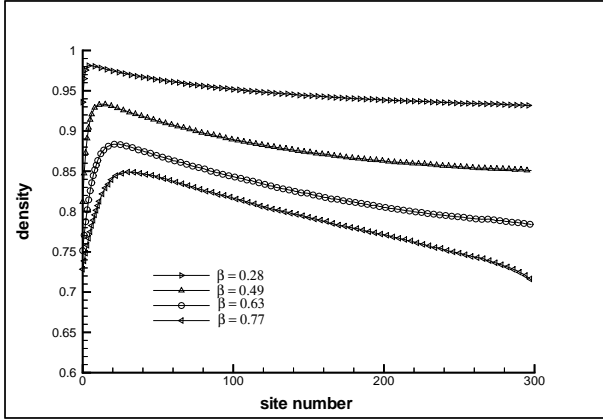


Fig. 14: density profile on the filament for various values of β for a system of size $Lx = 300$, $\alpha = 0.7$ and $\epsilon = 0.015$.

One observes that for large β a linear profile forms in the bulk. The effect of the left boundary on the profile is the formation of an increasing density layer. The location of the maximum point moves away the left boundary for higher β . One also observes a concave density profile structure for sufficiently small β . This aspect was absent

in $Lx = 100$ where not only the concavity did not exist but also for $\beta = 0.77$ there existed a concave profile. In order to have a deeper insight to the problem, we looked in more details into the effect of ϵ on the density profile. In the following figures, we show the density profile for some values of ϵ . α and β are fixed. We first consider the case $\alpha = \beta = 0.7$.

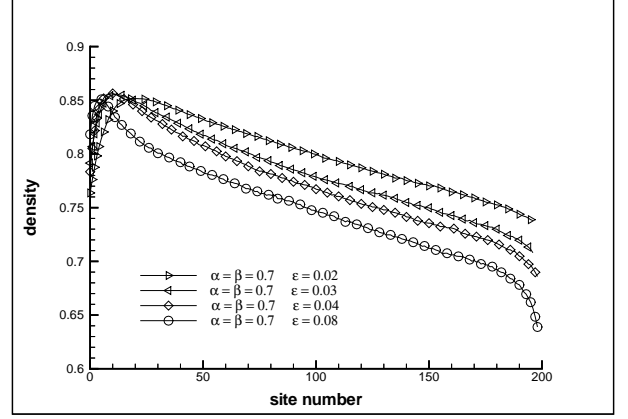


Fig. 15: density profile on the filament for various values of ϵ for a system of size $Lx = 200$, $Ly = Lz = 25$, $\alpha = 0.7$ and $\beta = 0.7$.

Except, a short region where the profile is increasing, we again observe a linearly decreasing profile. The overall effect of increasing ϵ is to reduce the density value throughout the chain. The reason for such decrease in the local densities could possibly be explained on account that in the present case $\alpha = \beta$ the system can maintain a large current therefore increasing ϵ would effectively reduces the number of bound particles and therefore the local density on the filament decreases. The next figure exhibits the density profile for the case $\alpha = \beta = 0.3$.

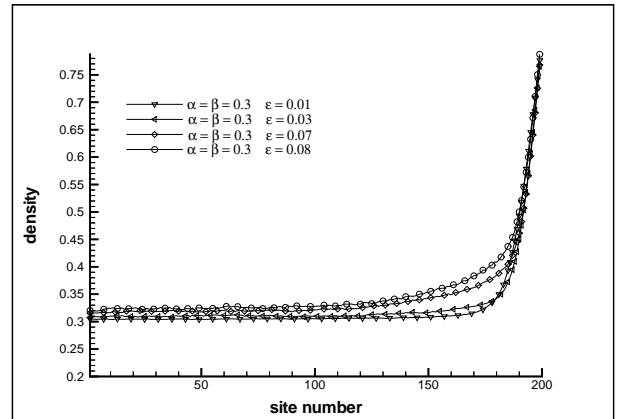


Fig. 16: density profile on the filament for various values of ϵ for a system of size $Lx = 200$, $Ly = Lz = 25$, $\alpha = 0.3$ and $\beta = 0.3$.

Here we observe a constant profile in the bulk accommodated with sharp increasing layer at the right boundary. This is also in contrast to ASEP where one expects a linear profile along the $\alpha = \beta \leq \frac{1}{2}$ line. We conclude that the detachment rate ϵ can give rise to significantly different features which are absent in ASEP. This conclusion has been earlier obtained for similar models without taking into account the dynamic of unbound particles^{15–18,32}. Our final graph depicts the density profile for some values of larger ϵ . α and β are fixed but unequal.

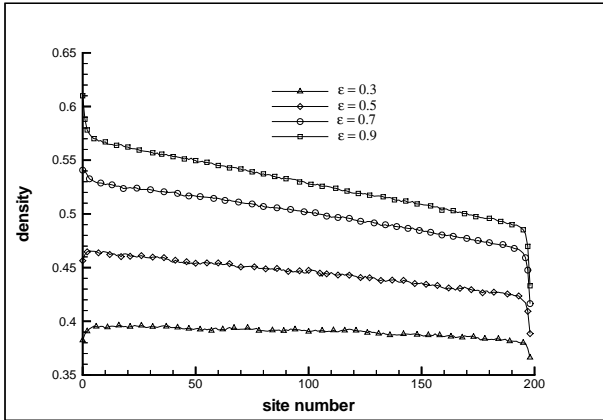


Fig. 17: density profile for various values of ϵ for a system of size $Lx = 200$, $Ly = Lz = 25$, $\alpha = 0.3$ and $\beta = 0.7$.

The above graph exhibits the profile in a low congestion state corresponding to $\alpha = 0.3$ and $\beta = 0.7$. As observed, the effect of ϵ is more notable for higher values. For small ϵ , the effect is an upward shift in the density profile. Larger ϵ not only shifts the density profile towards a higher value but also creates a slope in it. Finally, to see the effect of lateral dimensions of the compartment i.e., Ly and Lz , we performed extensive Monte Carlo simulations for $Ly = Lz = 12$ up to 70. Our results showed no significant changes for the case where ϵ is small.

IV. SUMMARY AND CONCLUDING REMARKS

Let us now summarize what has been done in this paper. We have developed a discrete time cellular automata model for the description of motor protein traffic through a filament-like track. Motors execute totally asymmetric random walk when bound onto the track. They randomly detach from the filament and perform unbiased random walk inside a closed compartment with reflecting boundary conditions. A similar problem has been earlier considered in²⁹. Our boundary condition and updating schemes is different to that in²⁹. Our main interest has been the interplay of the bulk and the boundary on the stationary properties of the system. In particular we

have studied the effect of varying the detachment rate ϵ on the transport characteristics of the model. Although the model behaviours resemble that of ASEP in some ranges of parameters, especially when the unbinding rate is sufficiently low, Our investigation has illustrated that for considerable high values of the unbinding rate, one observes remarkable distinct features with respect to ASEP. Specifically, the density profile shows linear and localized behaviour in some ranges of parameters. This implies that the density shock structure of the models should be entirely different than ASEP. This aspect can be of relevance to biological applications. Besides biological motivation, our study shed more lights onto the problem of bulk-boundary interplay in the transport characteristics of low dimensional non-equilibrium systems which recently has attracted the attention of researchers in the field. Analogous to the cases where the detachment/attachment rates are constant^{15–17}, we see the co-existence of high and low density regions which is termed *shock localization*. Moreover, we also observe other types of density structures such as linear density profiles with distinctive boundary behaviours. This shows that incorporating dynamics for the bulk particles, can drastically affect the phase structure of the system. It would be illustrative to find out the phase diagram structure of the model. This is our next step. Finally we recall that our model does not incorporate the internal degrees of freedom for motors. In practice, these motors resemble a two-headed creatures. Taking this fact into a quantitative description³⁶ together with chemical state of the motors are two crucial steps which should be considered in further progresses³⁷. Work along this line is in preparation and will be reported elsewhere.

V. ACKNOWLEDGEMENT

We highly wish to acknowledge the *Institute of Advanced Studies in Basic Sciences* (IASBS) for proving us with the computational facilities where the final stages of this work were carried out.

-
- ¹ T. Liggett in *Interacting Particle Systems: Contact, Voter and Exclusion Processes*, Springer, Berlin, (1999).
 - ² B. Schmittmann and R.K.P. Zia in: *Phase transitions and Critical Phenomena, vol 17*, ed. C. Domb and L. Lebowitz (London: Academic) 1995.
 - ³ G. Schütz in: *Phase transitions and Critical Phenomena, vol 19*, ed. C. Domb and L. Lebowitz, Academic Press, 2001.
 - ⁴ H. Hinrichsen, *Adv. Phys.*, **49**, 815, (2000).
 - ⁵ D. Chowdhury, L. Santen and A. Schadschneider, *Physics Reports*, **329**, 199 (2000).

- ⁶ D. Helbing, *Rev. Mod. Phys.*, **73**, 1067 (2001).
- ⁷ B. Kerner in *Physics of Traffic*, Springer, 2004.
- ⁸ J.T. MacDonald, J.H. Gibbs and A.C. Pipkin *Biopolymers*, **6**, 1 (1968); J.T. MacDonald and J.H. Gibbs *Biopolymers*, **7**, 707 (1969).
- ⁹ J. Krug *Phys. Rev. Lett.*, **67**, 1882 (1991).
- ¹⁰ B. Derrida, M.R. Evans, V. Hakim and V. Pasquier *J. Phys. A*, **26**, 1493 (1993).
- ¹¹ G. Schütz and E. Domany *J. Stat. Phys.*, **72**, 277 (1993).
- ¹² M.R. Evans, D.P. Foster, Godrèche and D. Mukamel *J. Stat Phys.*, **80**, 80 (1995).
- ¹³ A.B. Kolomeisky, G.M. Schütz, E.B. Kolomeisky and J.P. Straley *J. Phys. A*, **31**, 6911 (1998).
- ¹⁴ R.H. Fowler, *Statistical Mechanics*, Cambridge University Press, Cambridge (1936).
- ¹⁵ A. Parmeggiani, T. Franosch Th. E. Frey, *Phys. Rev. Lett.* **90**, 086601, 2003.
- ¹⁶ A. Parmeggiani, T. Franosch Th. E. Frey, *Phys. Rev. E* **70**, 046101, 2004.
- ¹⁷ M.R. Evans, R. Juhasz and L. Santen *Phys. Rev. E* **68**, 026117, 2003.
- ¹⁸ R. Juhasz and L. Santen *J. Phys. A* **37**, 3933, 2004.
- ¹⁹ J. Howard, *Mechanics of Proteins and the Cytoskeleton* (Sinauer Associates, Sunderland 2001).
- ²⁰ M. Schliwa, Editor, *Molecular Motors*, Wiley-VCH, Weinheim, (2003).
- ²¹ A. Ajdari, *Europhys. Lett.*, **31**, 69 (1995).
- ²² F. Jülicher, A. Ajdari and J. Prost *Rev. Mod. Phys.*, **69**, 1269 (1997).
- ²³ F. Nédélec, T. Surrey, A.C. Maggs and S. Leibler, *Nature*, **389**, 305 (1997).
- ²⁴ M.J. Schnitzer and S.M. Block *Nature*, **388**, 386 (1997).
- ²⁵ Y. Okada and N. Hirokawa *Science*, **283**, 1152 (1999).
- ²⁶ F. Nédélec, T. Surrey and A.C. Maggs, *Phys. Rev. Lett.*, **86**, 3192 (2001).
- ²⁷ R. Lipowsky, S. Klumpp and Th.M. Nieuwenhuizen, *Phys. Rev. Lett.* **87**, 108101, 2001.
- ²⁸ R. Lipowsky, S. Klumpp and Th. M. Nieuwenhuizen, *EuroPhys. Lett.* **58**, 468-474, 2002.
- ²⁹ S. Klumpp and R. Lipowsky, *J. Stat. Phys.* **113**, 233 (2003).
- ³⁰ R. Lipowsky, S. Klumpp and Th. M. Nieuwenhuizen, *EuroPhys. Lett.* **66**, 90, 2004.
- ³¹ R. Lipowsky, S. Klumpp and Th. M. Nieuwenhuizen, *Phys. Rev. E* **69**, 061911, 2004.
- ³² S. Klumpp, T. M. Nieuwenhuizen and R. Lipowsky, arXiv:q-bio.SC/0502024.
- ³³ S. Seiler, J. Kirchner, C. Horn, A. Kallipolitou, G. Wöhlke and M. Schliwa, *Nature Cell Biol.*, **2**, 333 (2000).
- ³⁴ L.S.B. Goldstein, Z. Yang, *Annu. Rev. Neurosci.*, **23**, 39 (2000).
- ³⁵ A.B. Dahlström, K.K. Pfister and S. T. Brady, *Acta. Physiol. Scand.*, **141**, 469 (1991).
- ³⁶ A.B. Kolomeisky and H. Phillip III, arXiv cond-mat/0503169
- ³⁷ K. Nishinara, Y. Okada, A. Schadschneider and D. Chowdhury, *Phys. Rev. Lett.*, **95**, 118101, 2005.